sustainability

MDPI

Article

Multi-State Car-Following Behavior Simulation in a Mixed Traffic Flow for ICVs and MDVs

Chengju Song and Hongfei Jia *

Transportation Collage, Jilin University, Changchun 130022, China
* Correspondence: jiahf@jlu.edu.cn; Tel.: +86-15663817336

Abstract: With the development of intelligent connected vehicles (ICVs) and communication technology, collaborative operation among vehicles will become the trend of the future. Thus, traffic flow will be mixed with manual driving vehicles and ICVs. A mixed traffic flow is a traffic flow state lying between autonomous and manual traffic flows. In order to describe the car-following characteristics in a mixed traffic flow, the cooperative adaptive cruise control (CACC) car-following model and the intelligent driver model (IDM) were adopted. The car-following characteristics of different platoons from these two car-following models were analyzed. The CACC mixing ratio was used to describe the mixed traffic flow. The fixed states and disturbance states of the car-following platoons were simulated. The fixed states can be divided into three categories: the steady state, acceleration state, and deceleration state. The effects of different car-following cases and different mixing ratios on mixed traffic flow in different states were discussed. The results show that (1) in the steady state with a smaller mixing ratio, the operating speed and traffic volume of the mixed traffic flow were positively correlated. The overall traffic volume decreased with the increase in the mixing ratio, and the gap gradually narrowed. At a larger mixing ratio, the operating speed and traffic volume were negatively correlated. The overall traffic volume increased with the increase in the mixing ratio. (2) In the acceleration state, the maximum traffic volume in the platoon and the optimal mixing ratio were linearly related to the acceleration. (3) In the deceleration state with a fixed mixing ratio, the traffic volume decreased with the increase in the deceleration, with slight differences in the changing trend of the volume of the mixed flow. Under disturbances, the mixed traffic volume was positively correlated with the mixing ratio, i.e., at a larger mixing ratio, the anti-interference ability of the mixed traffic flow was higher.

Keywords: traffic engineering; mixed traffic flow; simulation; car-following platoon; mixing ratio; traffic volume

Citation: Song, C.; Jia, H. Multi-State Car-Following Behavior Simulation in a Mixed Traffic Flow for ICVs and MDVs. *Sustainability* **2022**, *14*, 13562. https://doi.org/10.3390/su142013562

Academic Editors: Xiaoyuan Wang, Junyan Han and Gang Wang

Received: 1 September 2022
Accepted: 18 October 2022
Published: 20 October 2022

1. Introduction

Autonomous driving technology combines traffic monitoring, route navigation, artificial intelligence, and other technologies to achieve automatic computer control of vehicles. This technology has been studied for decades and has shown a trend toward practicality in recent years.

Autonomous driving technology can significantly prevent traffic accidents and reduce CO_2 emissions. It is predicted that global autonomous driving vehicle sales will account for 0.2% of the total vehicle sales in the next ten years and 9.2% in the next 20 years. Compared to the vehicle–infrastructure (V2I) collaboration technology, autonomous driving technology is less dependent on V2I communication environments. Thus, autonomous driving technology can be developed relatively independently and integrated into V2I collaboration systems as a basic terminal technology. Autonomous driving vehicles can acquire the surrounding traffic conditions through video cameras, radar sensors, and laser rangefinders installed on the vehicles, realize navigation through digital maps and global positioning systems, and achieve real-time control of vehicle driving status through

built-in intelligent algorithms. Therefore, compared to ordinary drivers, autonomous driving vehicles have more timely and accurate abilities to perceive traffic conditions, more stable and safer judgment and decision-making abilities, and more economical and environmentally friendly power output control.

The car-following behavior is one type of normal traffic flow behavior. The driving state varies greatly due to the driver's perception of the driving environment. It has been the goal of traffic practitioners to achieve a comprehensive, scientific, and accurate model description. Car-following theory is an important branch of traffic flow theory and is also the main theory for describing car-following behavior [1]. During car following, the rear vehicle determines the current driving decision based on the operating state of the front vehicle (e.g., the operating speed, acceleration, and distance, as well as the driver's characteristics). The traffic flow under autonomous driving conditions can achieve an excellent following state. There is a mixed traffic flow state between the manual driving state and the autonomous driving state, which consists of autonomous and manual driving vehicles.

In order to seize the technological development opportunities brought to China by intelligent transportation technology, China's autonomous vehicles and intelligent networked transportation systems have developed to a national strategic level. The connected and automated vehicle (CAV) industry is listed as one of the key areas in "Made in China 2025" (a national strategic plan and industrial policy of China) and the "14th Five-Year Plan". In China, the top-level design of autonomous driving has been strengthened. Documents such as the "Action Plan for the Development of the Intelligent Connected Vehicle Industry", "Intelligent Vehicle Innovation and Development Strategy" and "Guiding Opinions on Promoting the Development and Application of Road Traffic Autonomous Driving Technology" were issued to promote the development and application of autonomous driving technology. In July 2021, the "Management Specification for Road Test and Demonstration Application of Intelligent Connected Vehicles (Trial)" and the "Opinions on Strengthening the Administration of Access of Intelligent and Connected Vehicle Producers and Products" were released. In August 2022, the "Notice on the Pilot Application of High-precision Maps for Intelligent Connected Vehicles" was released to regulate the testing and application of autonomous vehicles. With the commercialization of 5G communication technology, CAVs can drive in a coordinated adaptive cruise control mode through vehicle-to-vehicle (V2V) communication technology, i.e., they are CACC. Real-world vehicle tests in actual road environments have shown that [2] the gradual popularization of CAVs is conducive to alleviating traffic congestion and improving traffic safety. Therefore, research on the characteristics of mixed traffic flow under mixed CACC conditions is of significance for future practical applications and has received extensive attention from scholars and engineers [3–5].

This paper is organized as follows. Following the introduction, Section 2 presents a review of the literature on relevant theoretical and simulation studies of car-following behavior for intelligent connected and manual driving vehicles. Section 3 introduces the car-following models. Section 4 presents the proposed car-following model for a mixed traffic flow and the simulation of car-following characteristics in different traffic flow states. Section 5 analyzes the mixed car-following flow characteristics in a disturbance state. Section 6 summarizes the main findings of this study.

2. Literature Review

International scholars generally believe that the application of autonomous driving technology can effectively reduce the delay of vehicles' responses to changes in surrounding traffic conditions and the time distance between vehicles. Thus, this can help improve the inherent characteristics of traffic flows and achieve a comprehensive breakthrough in traffic capacity, energy saving and emission reduction, and traffic safety. In this study, the literature is discussed from the following two perspectives.

2.1. Theoretical Studies

Many theoretical studies on car-following behavior have been conducted. Theoretical studies focus on hypotheses about a driver's response. The model designers generally propose various realistic theoretical hypotheses based on observations of car-following behavior, thus establishing car-following models. Drivers tend to choose acceptable strategies rather than optimal strategies due to insufficient experience or time. Current car-following models that consider human factors can be divided into models that consider perception thresholds [6,7], a driver's visual angles [8,9], risk perception [10,11], and distraction and errors [12,13]. For example, Ozkan et al. [14] used inverse reinforcement learning to model the unique car-following behaviors of different human drivers when interacting with CAVs and other human-driven vehicles. They also considered the energy efficiency and the heterogeneous characteristics of drivers' behaviors. In addition, the derivation of existing theoretical models and the application of new theories were also performed. Scholars have added new theoretical assumptions or informational factors to existing car-following models to continuously optimize the car-following process and maximize car-following efficiency. Current and new theoretical models include multi-interval car-following models [15,16], machine learning models [17,18], optimal control models [19–22], and extended-effect models [23,24].

Autonomous driving technology and V2V communication technology will induce the long-term mixed traffic flow of CAVs and regular vehicles in the future [25,26]. There are many theoretical studies on mixed traffic flow. For example, Qin [27] proposed a generalized framework of the Lighthill–Whitham–Richards (LWR) model for such mixed traffic flow at different CACC penetration rates. Three specific car-following models (i.e., the intelligent driver model (IDM) and the CACC and ACC models validated by the Partners for Advanced Transit and Highways (PATH) program) were selected as examples to investigate the propagation of small perturbations and shock waves.

2.2. Simulation Studies

The simulation research focuses on dynamic simulations that use car-following models to test the implementation of control strategies. Thus, these will provide a reference for formulating reasonable and safe control strategies. The simulation objects of available studies include theoretical models (e.g., a family of neural-network-based car-following models), designed physics-informed deep learning car-following model (PIDL-CF) architectures encoded with four popular physics-based models [28], traffic scenes (e.g., cautious, normal, and aggressive autonomous driving styles and their effects on important variables in traffic flow theory) [29], road networks with non-signalized intersections in a connected-vehicle environment [30], adaptive cruise control (ACC) systems for ACC vehicles [31], and novel cellular automata models for mixed traffic considering the limited visual distance to explore the influence of visibility capability and CAV market penetration on traffic efficiency [32].

Previous studies have shown that current research is still focused on describing and analyzing car-following behavior. However, the description of car-following behavior under mixed-traffic-flow conditions is inaccurate, and the analysis of different car-following states in a mixed traffic flow is lacking. Thus, it is necessary to further explore car-following models in mixed traffic flow. In this paper, a car-following model for a mixed traffic flow at different mixing ratios was established based on the classical car-following model. The operating characteristics of the mixed traffic flow under different car-following conditions were analyzed.

3. Description of Car-Following Models of Traffic Flows

In order to describe the behavior of autonomous/manual driving, selecting a suitable car-following model is necessary. This section presents the car-following model used to study the mixed traffic flow, the calibration process, and the simulation results. Model parameters are also recommended in order to provide a basis for subsequent mixed traffic flow modeling.

3.1. Autonomous Driving Model

The CACC model was selected as the autonomous driving model in this paper. This model uses vehicle-to-vehicle communication technology to realize real-time data transmission of the driving status parameters of the front vehicle and achieve feedback adjustment of the headway, operating speed, and acceleration in combination with the control parameters. Thus, the traffic flow can be continuously improved and managed. This is a hotspot in the current research on autonomous car-following control models, which can realize the overall optimization of traffic congestion, energy consumption, and emission.

The constant-headway car-following model proposed by the PATH Laboratory in Berkeley, California, is a more successful model application and is expressed as

$$\ddot{X}_{n+1}(t+T) = \alpha\ddot{X}_n(t) + \beta(X_n(t) - X_{n+1}(t) - t_g\dot{X}(t) - L - S_0) + \gamma(\dot{X}_n(t) - \dot{X}_{n+1}(t)) \quad (1)$$

where $\dot{X}_n(t)$ and $\dot{X}_{n+1}(t)$ are the velocities of the nth and the $(n+1)$th vehicle at the moment t, respectively; $\ddot{X}_{n+1}(t)$ and $\ddot{X}_n(t)$ are the accelerations of the nth vehicle and the $(n+1)$th vehicle at the moment t, respectively; $X_n(t)$ and $X_{n+1}(t)$ are the positions of the nth vehicle and $(n+1)$th vehicle at the moment t, respectively; t_g is the desired headway; L is the vehicle length; S_0 is the safe stopping distance; T is the reaction time; α, β, and γ are the coefficients to be determined.

The PATH laboratory at the University of California, Berkeley, integrated the CACC control system into four real-world vehicles. Actual trajectory data of the CACC vehicles were obtained, and the parameters of the CACC car-following model were calibrated. Their real-world vehicle tests showed that the calibrated model exhibited car-following characteristics consistent with those of actual vehicles. The parameter values [33] were also recommended: $\alpha = 1.0$, $\beta = 0.2$, and $\gamma = 3.0$. This model has a simple structure and explicit meaning, and it is the most commonly used car-following model based on constant headway.

3.2. Manual Driving Model

The IDM model was selected as the manual driving model. This model is one of the classical models for describing the car-following behavior in single-lane driving in different traffic flow states, with the advantages of good empirical conformity and easy calibration. The model is expressed as

$$\begin{gathered} \ddot{X}_{n+1}(t+T) = a\left(1 - \left(\frac{\dot{X}_n(t)}{v_0}\right)^{\delta} - \left(\frac{S_0 + \dot{X}_n(t)T + S^*}{X_n(t) - X_{n+1}(t) - L}\right)^2\right) \\ S^* = \frac{\dot{X}_n(t)(\dot{X}_n(t) - \dot{X}_{n+1}(t))}{2\sqrt{ab}} \end{gathered} \quad (2)$$

where a is the maximum acceleration; b is the comfortable deceleration; δ is the acceleration index; v_0 is the desired velocity in free flow conditions.

The data for the parameter calibration of the IDM model were obtained from the Next Generation Simulation (NGSIM) dataset. The calibration data were collected between 7:50 and 8:35 during the morning peak (45 min) on Route 101 in Los Angeles, CA, USA. The entire section was about 700 m long and included five main lanes and one additional lane. The data were extracted and processed according to certain rules, and 5687 two-vehicle car-following datasets (each with a 30 s duration) were obtained. The data were sampled, manually observed, and tested. No invalid data were found. Then, these data were used to calibrate the IDM model. The reasonable maximum optimal IDM parameters were obtained [34,35], as shown in Table 1.

Table 1. Parameter values of the IDM model.

Parameters	Typical Values	Parameters	Typical Values
a	1.0 m/s^2	S_0	2.0 m
b	2.0 m/s^2	L	5.0 m
δ	4.0	v_0	12 m/s
T	1.5 s		

4. Car-Following Characteristics of a Mixed Traffic Flow in the Fixed State

A platoon was built using the CACC and IDM car-following models. The platoon was arranged as follows: five vehicles; initial headway space, 20 m; initial platoon speed, 10 m/s. Considering a disturbance, the first vehicle in the platoon may accelerate or decelerate. In this paper, the disturbance function was taken as sinusoidal fluctuations in the changes in a vehicle's acceleration/deceleration in a stable state. The proposed disturbance function is expressed as

$$v = A\sin(\omega t) \tag{3}$$

where A indicates the acceleration amplitude of the first vehicle due to the disturbance, in m/s^2; ω indicates the angular frequency of the disturbance signal, in rad/s.

In this paper, considering driving comfort, the amplitude of disturbance A and ω were taken as 0.6 m/s^2 and 1 rad/s.

It is assumed that there are only two kinds of car-following behavior in the traffic flow, i.e., CACC and IDM, where the mixing ratio of CACC is p. The density of a mixed car-following flow can be expressed as

$$k_m = \frac{1}{ph_c + (1-p)h_i} \tag{4}$$

where h_c is the headway space in the CACC condition; h_i is the headway space in the IDM condition.

4.1. Car-Following Characteristics in the Stable State

When the mixed car-following flow reaches the stable state, the vehicle speed in the platoon is uniform and the vehicle acceleration is zero. The initial parameters were formulated as follows: initial headway space of the platoon, 50 m; the uniform speed of the platoon, 20, 25, and 30 m/s. Then, the traffic volume changes in the mixed car-following flow at different mixing ratios were simulated (Figure 1).

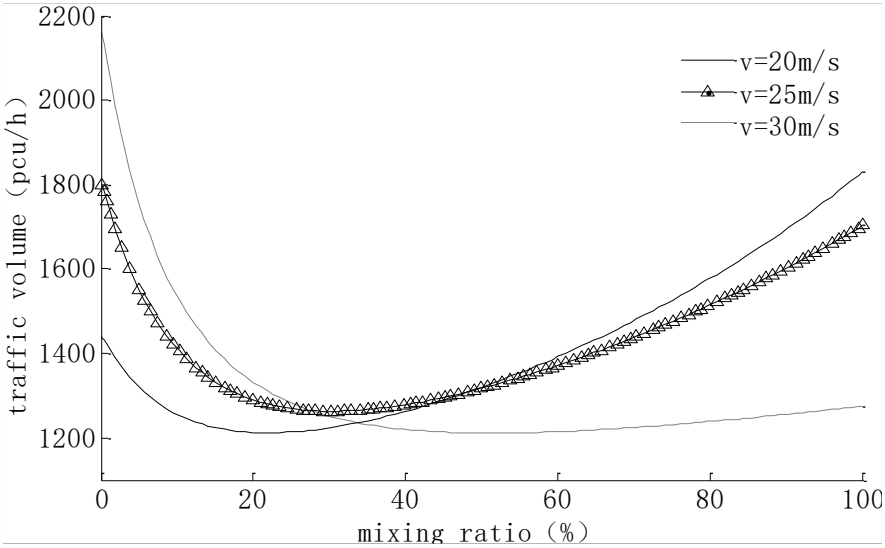

Figure 1. Changes in the mixed traffic volume at different mixing ratios.

From Figure 1, with the increase in the mixing ratio, the traffic volume in the mixed car-following flow showed a trend of first decreasing and then increasing. This was because the intelligent advantages of CACC vehicles could not be reflected at a low mixing ratio, and the V2V communication was discontinuous and unstable. These became disturbance factors for the car-following platoon. With the increase in the mixing ratio, the coordination efficiency of the CACC vehicles was significantly improved, thereby improving the running efficiency of the whole car-following platoon. Since the speed was constant, the curve's trend also reflected the change in the density of the car-following platoon. Corresponding to a certain equilibrium speed, the platoon density was the lowest when the mixing ratio was at the critical density, which is marked as p^*. When the mixing ratio was less than p^*, the platoon density and traffic volume decreased with the increase in the mixing ratio. When the mixing ratio was larger than p^*, the platoon density and traffic volume increased with the increase in the mixing ratio. Table 2 shows the four data groups at mixing ratios of 20%, 40%, 60%, and 80%, respectively.

Table 2. Comparison of the traffic volume at different speeds and different mixing ratios (unit: pcu/h).

Simulation Time / Speed (m/s)	20%	40%	60%	80%
20	1213	1263	1393	1579
25	1290	1279	1372	1516
30	1331	1220	1215	1239

From Table 2, compared to the traffic volume at the mixing ratio of 20%, the traffic volume at the mixing ratio of 80% increased by 23.2% and 14.9% at 20 and 25 m/s, respectively, while decreasing by 7.4% at 30 m/s.

In addition, with the increase in the equilibrium speed, the critical density p^* gradually increased. In contrast, in the steady state, the traffic volume corresponding to a high operating speed was higher at a lower mixing ratio. The traffic volume corresponding to a low operating speed was higher at a higher mixing ratio.

Similarly, with the increase in the speed from 20 to 30 m/s, the traffic volume increased by 8.9% at the mixing ratio of 20, while decreasing by 3.5%, 14.6%, and 27.4% at the mixing ratios of 40%, 60%, and 80%, respectively.

4.2. Car-Following Characteristics in the Acceleration State

In order to analyze the operating characteristics of the mixed car-following flow under the acceleration condition, three acceleration states were formulated in this paper. The initial speed was 10 m/s; the initial headway space was 20 m; the acceleration was set to 0.20, 0.25, and 0.30 m/s^2. The curves of the traffic volume changes in the mixed car-following flow are shown in Figure 2.

As shown in Figure 2, in the acceleration state, the traffic volume of the mixed car-following flow showed certain fluctuating characteristics, i.e., a decreasing–increasing–decreasing trend. The fluctuation was slight in the early stage and increased in the later stage. At a low mixing ratio, the traffic volume was positively correlated with the acceleration, without significant differences. At a high mixing ratio, the traffic volume was negatively correlated with the acceleration, with significant differences.

For a certain acceleration state, two traffic volume peaks occurred at different mixing ratios, i.e., p_1^* and p_2^*. When the mixing ratio was less than p_1^*, the traffic volume was negatively correlated with the mixing ratio. When the mixing ratio lay within $[p_1^*, p_2^*]$, the traffic volume was positively correlated with the mixing ratio. When the mixing ratio was greater than p_2^*, the traffic volume was negatively correlated with the mixing ratio.

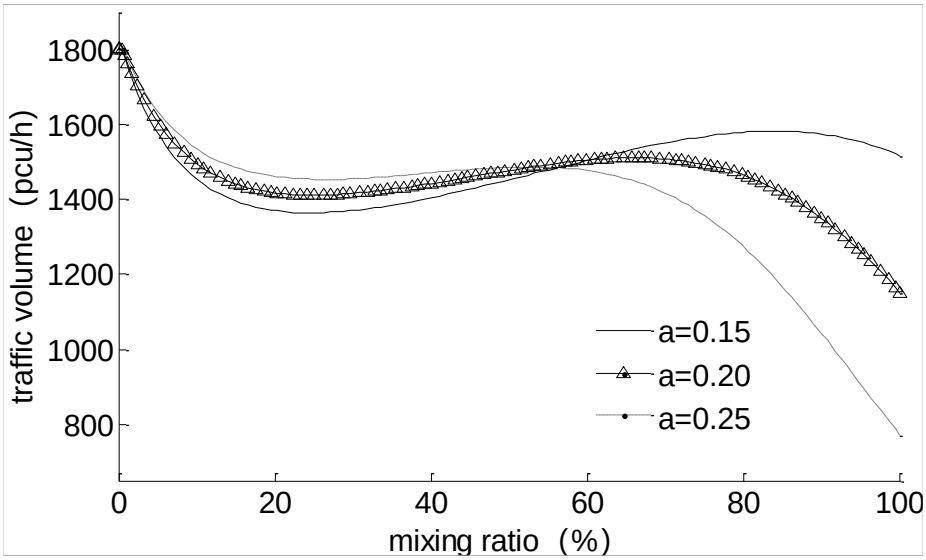

Figure 2. Relationship between the mixing ratio and traffic volume under different acceleration conditions.

The initial conditions were unchanged. The maximum traffic volume under different acceleration conditions with different mixing ratios is compared and summarized in Table 3.

Table 3. Parameter combinations under maximum traffic.

No.	Acceleration (m/s^2)	Optimal Mixing Ratio (%)	Maximum Traffic Volume (pcu/h)
1	0.18	93.77	1636
2	0.19	87.87	1606
3	0.20	84.39	1582
4	0.23	72.80	1531
5	0.25	66.49	1510
6	0.27	60.90	1497
7	0.30	53.18	1486
8	0.33	45.68	1485

The maximum traffic volume and the optimal mixing ratio were taken as the dependent variables, and the acceleration was an independent variable. The fitting equations can be expressed as:

$$\begin{cases} Q_{\max} = 1786.47 - 1004.48a (R^2 = 0.854) \\ r_{best} = 147.73 - 316.29a (R^2 = 0.987) \end{cases} \quad (5)$$

where $Q_{\max}$ is the maximum traffic volume, a is the acceleration of the platoon, and r_{best} is the optimal mixing ratio.

Since $r_{best} \leq 100$, it can be determined that $a \geq 0.15$, i.e., when the acceleration $a < 0.15$, the curve of the change in the mixing ratio and traffic volume had a single-peaked characteristic.

4.3. Car-Following Characteristics in the Deceleration State

Similarly, in order to analyze the operating characteristics of the mixed car-following flow under deceleration conditions, three deceleration states were simulated in this paper. The initial speed and initial headway space were 30 m/s and 100 m, respectively. The decelerations were set to -0.15, -0.20, and -0.25 m/s^2, respectively. The curves of the changes in the traffic volume of the mixed car-following flow are shown in Figure 3.

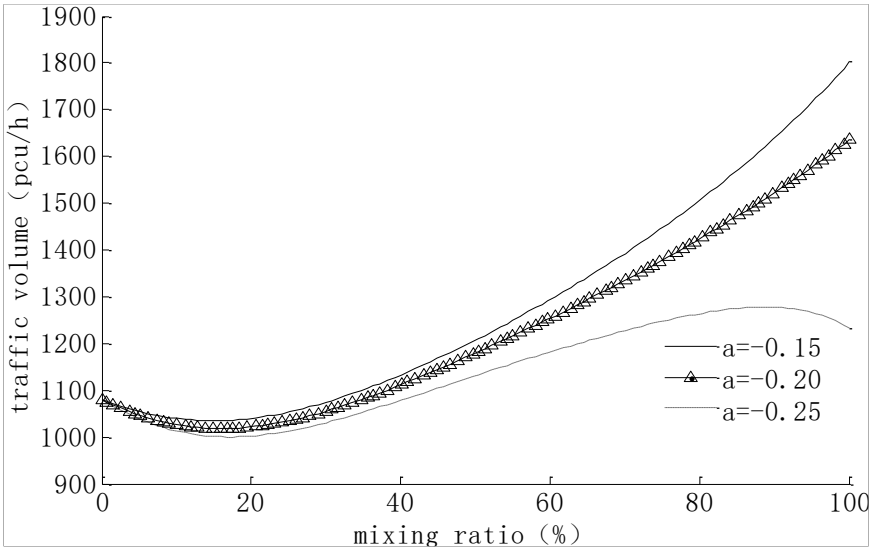

Figure 3. Relationship between the mixing ratio and traffic volume under different deceleration conditions.

As shown in Figure 3, at the same mixing ratio, the traffic volume decreased with the increase in deceleration, with a slight difference in the changing trend. At a small deceleration, the traffic volume showed a trend of first decreasing and then increasing with the increase in the mixing ratio. When the deceleration exceeded a certain value, the traffic volume showed a decreasing–increasing–decreasing trend with the increase in the mixing ratio. In particular, at a larger mixing ratio, the reduction rate was higher.

The data points at the mixing ratios of 20%, 40%, 60%, and 80% were extracted, as shown in Table 4.

Table 4. Comparison of the traffic volume at different decelerations and different mixing ratios (unit: pcu/h).

Deceleration (m/s^2) \ Mixing Ratio	20%	40%	60%	80%
0.15	1040	1133	1295	1507
0.20	1022	1112	1255	1425
0.25	1002	1079	1182	1264

The traffic volume at the mixing ratio of 20% was taken as the baseline value. As shown in Table 4, the traffic volume at the mixing ratio of 80% increased by 31.0%, 28.3%, and 20.7% at the deceleration rates of 0.15, 0.20, and 0.25 m/s^2, respectively.

Similarly, with the increase in the deceleration from 0.15 to 0.25 m/s^2, the traffic volume of the mixed car-following flow decreased by 3.8%, 5.0%, 6.2%, and 19.2% at 20%, 40%, 60%, and 80%, respectively.

5. Analysis of the Characteristics of the Mixed Car-Following Flow in the Disturbance State

It has been shown that fixed traffic compositions and car-following states significantly impact the car-following effect. However, the interpretation of microscopic car-following behaviors still needs to be further studied. This section discussed the microscopic car-following effects and the effects of mixing ratios on the car-following platoon to explain the microscopic behavior of the mixed traffic flow.

5.1. Car-Following Effects in Different Cases

According to the dynamic characteristics of traffic flows, the relative spatial positions of vehicles in a mixed traffic flow are random. Therefore, in a mixed traffic flow composed of CACC and IDM, four cases may occur in a car-following platoon:

Case 1: CACC vehicles are followed by IDM vehicles;
Case 2: CACC vehicles are followed by CACC vehicles;
Case 3: IDM vehicles are followed by CACC vehicles;
Case 4: IDM vehicles are followed by IDM vehicles.

Referring to the abovementioned calibration data, the acceleration disturbance from Equation (3) was used as the disturbance condition for the lead vehicle in the assumed car-following platoon to simulate and analyze the car-following effects in different cases, as shown in Figure 4.

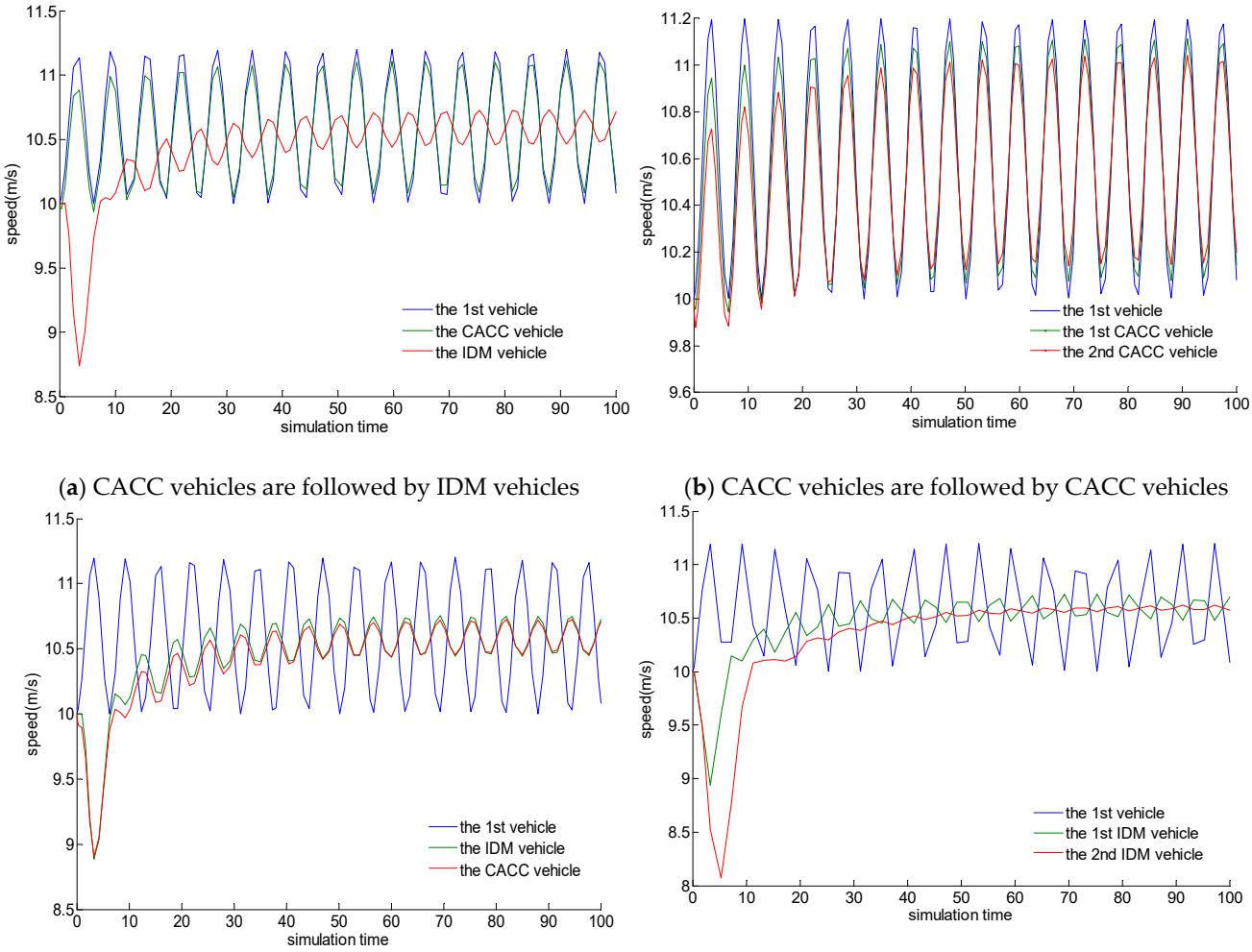

(**a**) CACC vehicles are followed by IDM vehicles

(**b**) CACC vehicles are followed by CACC vehicles

(**c**) IDM vehicles are followed by CACC vehicles

(**d**) IDM vehicles are followed by IDM vehicles

Figure 4. Car-following effects in different cases.

Figure 4 shows the changes in speed of various types of vehicles in different cases. The CACC vehicle had a significantly better car-following ability and could follow the lead vehicle with smaller speed differences, better speed conditions, and higher adaptability. The IDM vehicle was almost synchronized with the lead vehicle in terms of the speed-change curve and showed relatively smooth car-following behavior. The IDM vehicle also reacted roughly to the speed fluctuation of the lead vehicle, with increasing speed adaptability.

5.2. Car-Following Effects at Different Mixing Ratios

Under realistic conditions, the probability that a car-following platoon maintains a fixed state is low. Commonly, a car-following platoon shows fluctuating states due to various disturbances. In this paper, the disturbance function in Equation (3) was imposed, assuming that the disturbance function was sinusoidal, the acceleration $A = 0.6$, and the disturbance frequency $\omega = 0.2$.

In this paper, the initial speed of the car-following platoon was 10 m/s and the initial headway space was 50 m. The changes in the states of the mixed car-following flow at the mixing ratios of 20%, 50%, and 80% were simulated. Figure 5 shows that the traffic volume of the mixed car-following flow fluctuated synchronously with the disturbance. With the increase in the mixing ratio, the traffic volume of mixed car-following flow increased accordingly. It was also found that the mixed car-following flow with different mixing ratios reached the maximum value at the simulation times of 15, 46, and 77, respectively. The corresponding maximum values are shown in Table 5.

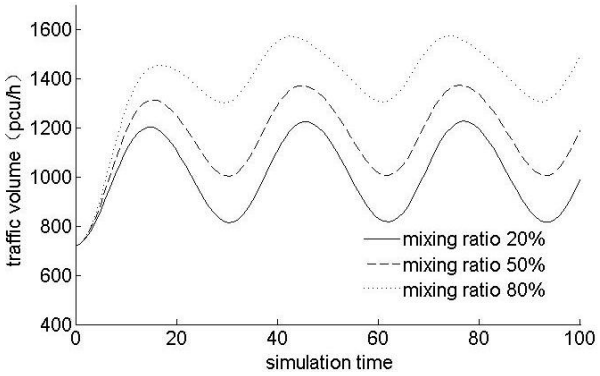

Figure 5. Changes in the mixed traffic flow with different mixing ratios.

Table 5. Summary of the maximum values at different mixing ratios (unit: pcu/h).

Mixing Ratio \ Simulation Time	15	46	77	Relative Changing Rate
20%	1202	1222	1227	2.0%
50%	1313	1365	1371	4.2%
80%	1451	1566	1570	7.6%

As can be seen in Table 5, the relative rates of change at the mixing ratios of 80%, 50%, and 20% were 7.6%, 4.2%, and 2.0%, respectively. This indicates that at a higher mixing ratio, the mixed traffic flow showed a larger relative rate of change. This may suggest that a mixed car-following flow can significantly increase the traffic volume and resist disturbances better when the mixing ratio is high.

6. Conclusions

In this paper, the car-following characteristics of a mixed traffic flow in different fixed states and mixing ratios were simulated and analyzed by using the CACC and IDM models.

(1) In the steady state, the mixed car-following traffic volume decreased and then increased with the increase in the mixing ratio. The trends of the changes were inconsistent at different mixing ratios.

(2) In the acceleration state, the maximum mixed car-following traffic volume and the optimal mixing ratio were linearly related to the acceleration.

(3) In the deceleration state, the maximum mixed car-following traffic volume and the deceleration speed tended to first decrease and then increase.

(4) Under disturbance conditions, CACC vehicles were able to better adapt to the fluctuations of the lead vehicle, with significantly greater speed adjustment abilities. In

contrast, the speed adjustments of IDM vehicles during car following were relatively rough. In addition, the mixed car-following traffic volume was positively correlated with the mixing ratio. At a higher mixing ratio, the mixed car-following flow had a stronger resistance to disturbances.

Author Contributions: The authors confirm contribution to the paper as follows: methodology and software, C.S.: project administration and funding acquisition, H.J. All authors have read and agreed to the published version of the manuscript.

Funding: This research was funded by the National Natural Science Foundation of China (Grant No.52072143); the Fundamental Research Funds for the Central Universities of China (Grant No.2572020BG02); University Nursing Program for Young Scholars with Creative Talents in Heilongjiang Province (Grant No.UNPYSCT-2018090); the Fundamental Research Funds for the Central Universities, CHD (Grant No.300102210523); and Fundamental Research Funds for the Provincial-Level Colleges and Universities in Heilongjiang Province (Grant No.2018CX08), And The APC was funded by the National Natural Science Foundation of China (Grant No.52072143).

Institutional Review Board Statement: Not applicable.

Informed Consent Statement: Not applicable.

Data Availability Statement: All data included in this study are available upon request by contact with the corresponding author.

Acknowledgments: The authors gratefully acknowledge support from the National Natural Science Foundation of China (52072143); the Fundamental Research Funds for the Central Universities (2572020BG02), the University Nursing Program for Young Scholars with Creative Talents in Heilongjiang Province (UNPYSCT-2018090), the Fundamental Research Funds for the Central Universities, CHD(300102210523), and Fundamental Research Funds for the Provincial-Level Colleges and Universities in Heilongjiang Province (2018CX08).

Conflicts of Interest: The authors declare no conflict of interest.

References

1. Yang, L.H.; Zhang, C.; Chou, X.-Y.; Li, S.; Wang, H. Research progress on car-following model. *J. Traffic Transp. Eng.* **2019**, *19*, 125–138.
2. Zhang, L.; Wang, Y.; Zhu, H. Theory and Experiment of Cooperative Control at Multi-Intersections in Intelligent Connected Vehicle Environment: Review and Perspectives. *Sustainability* **2022**, *14*, 1542. [CrossRef]
3. Zhong, Z.; Lee, J. The effectiveness of managed lane strategies for the near-term deployment of cooperative adaptive cruise control. *Transp. Res. Part A Policy Pract.* **2019**, *129*, 257–270. [CrossRef]
4. Navas, F.; Milanés, V. Mixing V2V- and non-V2V-equipped vehicles in car following. *Transp. Res. Part C Emerg. Technol.* **2019**, *108*, 167–181. [CrossRef]
5. Peng, Z.; Zhu, H.; Zhou, Y. Modeling cooperative driving strategies of automated vehicles considering trucks' behavior. *Phys. A Stat. Mech. Its Appl.* **2021**, *585*, 126386.
6. Hiroyuki; Konda; Hideki; Nakamura. Examination on Measuring Quality of Service Considering Car-Following Condition on Intercity Expressways. *JSTE J. Traffic Eng.* **2020**, *6*, A_9–A_15.
7. Guo, Y.; Zhang, Z.; Yuan, W.; Wang, C.; Wu, F.; Liu, Z. Accelerated Failure Time Model to Explore the Perception Response Times of Drivers in Simulated Car-Following Scenarios. *J. Adv. Transp.* **2020**, *2020*, 8894162. [CrossRef]
8. Jiang, N.; Yu, B.; Cao, F.; Dang, P.; Cui, S. An extended visual angle car-following model considering the vehicle types in the adjacent lane. *Phys. A Stat. Mech. Its Appl.* **2021**, *566*, 125665. [CrossRef]
9. Guan, X.; Cheng, R.; Ge, H. Bifurcation analysis of visual angle model with anticipated time and stabilizing driving behavior. *Chin. Phys. B* **2022**, *31*, 15. [CrossRef]
10. Huda, L.N.; Ismail, S. The effect of car drivers risk perception and driving behaviour towards accident risk: A case study. *IOP Conf. Ser. Mater. Sci. Eng.* **2020**, *801*, 012066. [CrossRef]
11. Wu, B.; Yan, Y.; Ni, D.; Li, L. A longitudinal car-following risk assessment model based on risk field theory for autonomous vehicles. *Int. J. Transp. Sci. Technol.* **2021**, *10*, 60–68. [CrossRef]
12. Muhrer, E.; Vollrath, M. The effect of visual and cognitive distraction on driver's anticipation in a simulated car following scenario. *Transp. Res. Part F Traffic Psychol. Behav.* **2011**, *14*, 555–566. [CrossRef]
13. Zatmeh-Kanj, S.; Toledo, T. Car Following and Microscopic Traffic Simulation Under Distracted Driving. *Transp. Res. Rec.* **2021**, *2675*, 643–656. [CrossRef]

14. Ozkan, M.F.; Ma, Y. Modeling Driver Behavior in Car-Following Interactions with Automated and Human-Driven Vehicles and Energy Efficiency Evaluation. *IEEE Access* **2021**, *9*, 64696–64707. [CrossRef]
15. An, S.; Xu, L.; Qian, L.; Chen, G.; Luo, H.; Li, F. Car-following model for autonomous vehicles and mixed traffic flow analysis based on discrete following interval. *Phys. A Stat. Mech. Its Appl.* **2020**, *560*, 125246. [CrossRef]
16. Zhang, J.; Liu, M.; Sun, Z. A Modified Mixed Car-following Model Considering that the Connected and Intelligent Vehicle and Non-connected Vehicle. *J. Phys. Conf. Ser.* **2021**, *1910*, 012019. [CrossRef]
17. Yan, X.H.; Zhou, Z.W. A Car-Following Model Using Online Sequential Extreme Learning Machine. *J. Phys. Conf. Ser.* **2021**, *1848*, 012095. [CrossRef]
18. Pan, Y.; Wang, Y.; Miao, B.; Cheng, R. Stabilization Strategy of a Novel Car-Following Model with Time Delay and Memory Effect of the Driver. *Sustainability* **2022**, *14*, 7281. [CrossRef]
19. Kanagaraj, V.; Treiber, M. Self-driven particle model for mixed traffic and other disordered flows. *Phys. A Stat. Mech. Its Appl.* **2018**, *509*, 1–11. [CrossRef]
20. Zhu, W.X.; Zhang, H.M. Analysis of feedback control scheme on discrete car-following system. *Phys. A Stat. Mech. Its Appl.* **2018**, *503*, 322–330. [CrossRef]
21. Zhai, C.; Wu, W. Car-following model based delay feedback control method with the gyroidal road. *Int. J. Mod. Phys. C* **2019**, *30*, 1950073. [CrossRef]
22. Chu, H.; Guo, L.; Yan, Y.; Gao, B.; Chen, H. Self-Learning Optimal Cruise Control Based on Individual Car-Following Style. *IEEE Trans. Intell. Transp. Syst.* **2020**, *22*, 6622–6633. [CrossRef]
23. Ma, M.; Xiao, J.; Liang, S.; Hou, J. An extended car-following model accounting for average optimal velocity difference and backward-looking effect based on the Internet of Vehicles environment. *Mod. Phys. Lett. B* **2022**, *36*, 2150562. [CrossRef]
24. Koh, M.; Ramírez, A.; Sipahi, R. Sub-platooning via Agent Separation for Improved Traffic Flow Metrics in a Car-Following Model. *Account. Constraints Delay Syst.* **2022**, *12*, 71–85.
25. Wang, Y.; Xu, R.; Zhang, K. A Car-Following Model for Mixed Traffic Flows in Intelligent Connected Vehicle Environment Considering Driver Response Characteristics. *Sustainability* **2022**, *14*, 11010. [CrossRef]
26. Xie, D.F.; Zhao, X.M.; He, Z. Heterogeneous Traffic Mixing Regular and Connected Vehicles: Modeling and Stabilization. *IEEE Trans. Intell. Transp. Syst.* **2018**, *20*, 1–12.
27. Qin, Y.; Wang, H.; Ni, D. LWR Model for Traffic Flow Mixed with CACC Vehicles. *Transp. Sci.* **2021**, *55*, 815–967. [CrossRef]
28. Mo, Z.; Shi, R.; Di, X. A physics-informed deep learning paradigm for car-following models. *Transp. Res. Part C Emerg. Technol.* **2021**, *130*, 103240. [CrossRef]
29. Lu, Q.L.; Qurashi, M.; Varesanovic, D.; Sodnik, J.; Antoniou, C. Exploring the influence of automated driving styles on network efficiency. *Transp. Res. Procedia* **2021**, *52*, 380–387. [CrossRef]
30. Chen, X.; Xu, B.; Qin, X.; Bian, Y.; Hu, M.; Sun, N. Non-signalized Intersection Network Management with Connected and Automated Vehicles. *IEEE Access* **2020**, *8*, 122065–122077. [CrossRef]
31. Li, Y.; Piao, C. Research on Adaptive Cruise Control Car-following Model Based on Dynamic Spacing in V2X Scenario. *J. Phys. Conf. Ser.* **2022**, *2246*, 012075. [CrossRef]
32. Gong, B.; Wang, F.; Lin, C.; Wu, D. Modeling HDV and CAV Mixed Traffic Flow on a Foggy Two-Lane Highway with Cellular Automata and Game Theory Model. *Sustainability* **2022**, *14*, 5899. [CrossRef]
33. Milanes, V.; Shladover, S.E. Modeling cooperative and autonomous adaptive cruise control dynamic responses using experimental data. *Transp. Res. Part C Emerg. Technol.* **2014**, *48*, 285–300. [CrossRef]
34. Yang, L.X.; Zhao, X.M.; Zheng, J.F. Correlations among Various Parameters in Car-Following Models with NGSIM Trajectory Data. *Appl. Mech. Mater.* **2011**, *66*, 179–184. [CrossRef]
35. Qin, Y.Y.; Wang, H.; Wang, W.; Wan, Q. Stability analysis and fundamental diagram of heterogeneous traffic flow mixed with cooperative adaptive cruise control. *Acta Phys. Sin.* **2017**, *66*, 252–261.